Chemical Science

ROYAL SOCIETY OF CHEMISTRY

EDGE ARTICLE

View Article Online
View Journal | View Issue

Cite this: *Chem. Sci.*, 2021, **12**, 6188

All publication charges for this article have been paid for by the Royal Society of Chemistry

Mechanically compliant single crystals of a stable organic radical†

Patrick Commins, [a] A. Bernard Dippenaar, [b] Liang Li, [a] Hideyuki Hara,[c] Delia A. Haynes *[b] and Panče Naumov *[a]

Mechanically compliant organic crystals are the foundation of the development of future flexible, light-weight single-crystal electronics, and this requires reversibly deformable crystalline organic materials with permanent magnetism. Here, we report and characterize the first instance of a plastically bendable single crystal of a permanent organic radical, 4-(4′-cyano-2′,3′,4′,5′-tetrafluorophenyl)-1,2,3,5-dithiadiazolyl. The weak interactions between the radicals render single crystals of the β phase of this material exceedingly soft, and the S–N interactions facilitate plastic bending. EPR imaging of a bent single crystal reveals the effect of deformation on the three-dimensional spin density of the crystal. The unusual mechanical compliance of this material opens prospects for exploration into flexible crystals of other stable organic radicals towards the development of flexible light-weight organic magnetoresistance devices based on weak, non-hydrogen-bonded interactions in molecular crystals.

Received 2nd March 2021
Accepted 26th March 2021

DOI: 10.1039/d1sc01246k

rsc.li/chemical-science

Introduction

'Soft crystal' is an emerging concept in materials research that combines two seemingly diametrically opposed ideas—*crystals*, which are normally hard and structurally ordered entities, and *soft* matter, a term which usually refers to disordered materials such as polymers, colloids, liquid crystals, and gels. Since the early days of structural elucidation of soft crystals[1–3] the unexpected contrast between the structure and physical properties of these paradoxical materials has drawn the attention of researchers towards understanding their mechanically compliant nature and its relation to the long-range structural order brought about by their crystal lattice.[4–6] Unlike inorganic materials such as metals, alloys and ceramics, most soft crystals are organic and have the important advantage of being comparably lighter in weight. Based upon the primary macroscopic deformation that is observed upon application of non-uniform mechanical pressure[7] they can be qualified as *elastic*, where the crystal fully recovers from the deformation, or *plastic*, where it experiences a permanent deformation. The initial concerns around whether plastic and elastic crystals retain their crystallinity through deformation have been recently dispelled.[7,8] The prospects for utility of soft crystals as light-weight optoelectronic elements in photonics,[9–13] sensing technology, actuation[14,15] and other applications that require smart materials[16–18] have resulted in an extensive search for new candidates and exploration of the multifaceted properties of this new materials class.[16–24] The past attempts to understand the chemical interactions that are required for plasticity or elasticity proposed that presence of slip planes,[4,25] hydrogen bonding,[26,27] π-interactions,[28,29] as well as quasiorthogonal strong and weak interactions[30] in the respective crystal structures may be relevant to the observed flexibility, although exceptional cases have also been reported.[31] While the debate on the critical structural factors that determine these properties is ongoing, many soft crystals continue to be discovered and reported, and they are now seen as an emerging distinct class of soft, ordered engineering materials.

As part of an ongoing structural exploration of stable thiazolyl radicals by one of our research teams, we recently observed that crystals of the stable dithiadiazolyl (DTDA) radical 4-(4′-cyano-2′,3′,4′,5′-tetrafluorophenyl)-1,2,3,5-dithiadiazolyl (**1**) (Fig. 1A) are mechanically compliant and can be easily bent without disintegration when they are pressed perpendicular to their longest axis. This material, whose crystal structure was first reported in 1995,[32] was the first DTDA radical to retain its paramagnetic nature in the solid state. It crystallizes as two polymorphs; the α phase (**1α**) exhibits short-range weak antiferromagnetic interactions at low temperature, whereas the β phase (**1β**) exhibits weak ferromagnetism (canted antiferromagnetism) at 36 K at ambient pressure. The ordering temperature of the β phase increases to 70 K under pressure.[33] The remarkable properties of **1** continue to generate interest,[34–37] and recently the conditions to selectively prepare either the α or the β phase have been reported.[38] We note that an

[a]*Smart Materials Lab, New York University Abu Dhabi, PO Box 129188, Abu Dhabi, United Arab Emirates. E-mail: pance.naumov@nyu.edu*

[b]*Department of Chemistry and Polymer Science, Stellenbosch University, P. Bag X1, Matieland, 7602, Republic of South Africa*

[c]*Bruker K.K., 3-9, Moriya, Kanagawa, Yokohama, Kanagawa 221-0022, Japan*

† Electronic supplementary information (ESI) available. See DOI: 10.1039/d1sc01246k

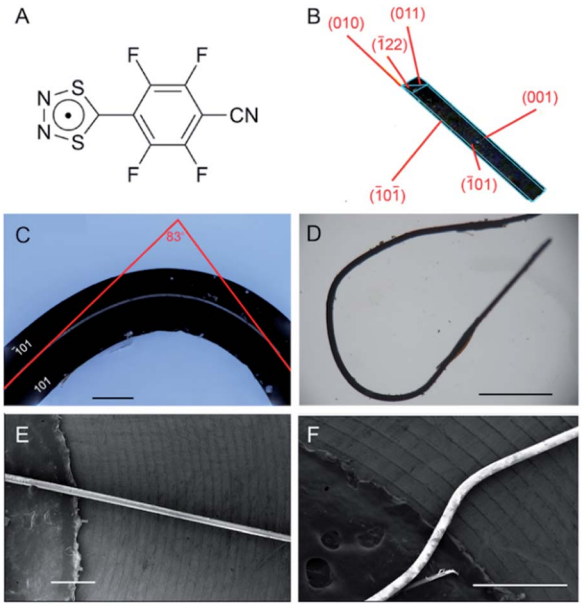

Fig. 1 Appearance and mechanical compliance of crystals of **1β**. (A) Chemical structure of 4-(4′-cyano-2′,3′,4′,5′-tetrafluorophenyl)-1,2,3,5-dithiadiazolyl, **1**. (B) Face indices of a crystal of **1β** with the faces outlined in cyan. (C and D) Optical images of crystals of **1β** bent to 83° (C) and to nearly a closed loop (314°) (D). (E and F) SEM images of a crystal of **1β** before (E) and after (F) bending. Scale bars: panel C, 100 μm; panel D, 1 mm; panels E and F, 500 μm.

early report[34] on **1** mentions that the crystals of **1β** are plastically deformable, although like many interesting observations, this result was not thoroughly investigated.

The crystal structures and packing motifs of DTDAs have been studied in detail.[39] Although plastic deformation has been reported for a number of diamagnetic crystals and other radicals,[40–43] it has not been investigated yet in a crystal of a stable neutral radical. Moreover, **1β** is the only bendable DTDA that has been identified to date. Based on a combination of crystallographic, mechanical and electron paramagnetic resonance (EPR) spectroscopic analysis, here we report details of the mechanical compliance of this radical crystal. We also demonstrate the role of F–π and S–N interactions in facilitating plastic bending, and expand the list of intermolecular interactions capable of generating soft crystals.

Results and discussion

The DTDA **1** was synthesized using a well-established one-pot procedure.[44] The crude radical was purified by sublimation under reduced pressure (~0.6 mbar line pressure) at 373–383 K to afford opaque, deep-red acicular crystals (Fig. 1B–D). The crystals are relatively stable, and can be kept under ambient conditions in air for approximately 12 hours before significant deterioration is observed. As the compound degrades, the crystals lose their luster and become brittle. The DSC of **1β** profile is shown in ESI Fig. S1.† The reflective faces (1̄01) and (101) are easily observed and provide a convenient way to detect cracking or dislocations during bending (Fig. 1C). The crystals are remarkably flexible and can be plastically bent and eventually even closed into a loop (Fig. 1D). Scanning Electron Microscopy (SEM) images of a crystal before (Fig. 1E) and after bending (Fig. 1F) complement the optical images and provide better resolution of the (1̄01)/(101) faces, showing that they remain pristine and undisturbed throughout the bent region. A single crystal that has been bent at an angle of 83° by applying pressure on its (1̄01) face is shown in Fig. 1C. It is worth noting that the degree of bending a crystal can withstand without cracking is directly related to the amount of time that had passed since it was sublimed. Freshly grown crystals have nearly pristine facets throughout the mechanical deformation (Fig. 1D), whereas aged crystals show cracks orthogonal to the crystal surface at the location of the highest bending angle (ESI Fig. S2†).

Crystals of **1** were freshly sublimed under reduced pressure at 373 K for 3 h, and were analyzed using single crystal X-ray diffraction. The determined structure is in agreement with the previously published structure of polymorph β (Fig. 2).[27] The most prominent intermolecular interaction in the structure is between the cyano functionality and the sulfur atoms of the

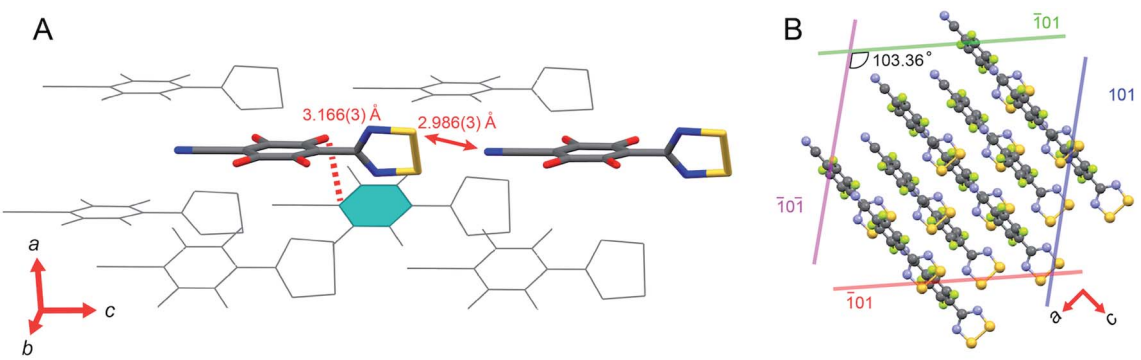

Fig. 2 Crystal structure of **1β** showing the relevant intermolecular interactions. (A) Relevant intermolecular interactions between the radical molecules, including the S–N interaction. (B) Packing of the radicals in the structure viewed down the *b* axis. The structural details were extracted from the crystal structure[34] of **1β** retrieved from the Cambridge Structure Database (CSD) (reference: YOXMUT01).

DTDA (2.986(3) Å), which links molecules into infinite head-to-tail chains that run along the *c* axis (Fig. 2A). Although the compound is a small aromatic molecule, the structure is noticeably devoid of strong π–π interactions. However, considering that the aromatic ring is tetraflourinated and substituted with cyano and dithiadiazolyl functional groups, most of the electron density of the ring is inductively pulled towards the periphery, which accounts for the lack of significantly strong π-stacking interactions. Instead, F–π interactions are observed within the structure, with an F-to-plane distance of 3.166(3) Å (Fig. 2A), which is close to similar distances reported in other perfluorinated aromatic compounds (3.0–3.14 Å).[45]

The ability of the crystal of **1β** to undergo two-dimensional plastic bending on both the (101) and ($\bar{1}$01) faces can be rationalized by examining the crystal structure of the unbent crystal.[34] The (101) and ($\bar{1}$01) faces are related by symmetry (Fig. 2B). Upon bending of the crystal on the (101)/($\bar{1}$01) face, the molecules can move along the glide planes parallel to the π-system and break and reform the weak F–π interactions, thereby effectively dissipating the mechanical stress (Fig. 2B). The π-system however is not parallel to the ($\bar{1}$$\bar{1}$01) plane and there is a 103.4° angle between the (101) and ($\bar{1}$$\bar{1}$01) face, so when force is applied on the ($\bar{1}$$\bar{1}$01) face the S–N interactions are also utilized to accommodate the deformation. As the crystal bends, the F–π interactions keep the molecules stacked in planes, while the S–N interactions maintain the integrity of the one-dimensional chains of molecules. Their combination allows the crystal to bend plastically. The separation and restoration of weak bonds is a common pattern in plastically bendable crystals. It has been observed previously with halogen bonds or interactions in hexachlorobenzene,[30] hexabromobenzene,[5] and *N*-(4-ethynylphenyl)-3-fluoro-4-(trifluoromethyl)benzamide.[46] To our knowledge, **1** is the first example of a bendable crystal whose molecules interact *via* F–π or S–N interactions. These results indicate that even though similar motifs such as slip planes are commonly utilized to generate dislocations during bending, the interactions that define those slip planes can be varied. This mechanism is consistent with those established for other plastically bendable crystals.[7,46,47]

The crystals of **1β** were found to be notably soft when touched with a hard object, and this softness may play a role in the observed plasticity. The mechanical properties of a freshly sublimed crystal on its (101)/($\bar{1}$01) faces were quantified using a tensile tester equipped with a three-point bending apparatus (Fig. 3). The results from five other crystals that were tested in the same manner are shown in the ESI Fig. S3.† At strain of up to 1.15% the crystal deforms elastically, as indicated by the linear portion of the stress–strain curve. When the strain exceeds 1.15% the crystal deforms plastically, and ultimately yields at a stress of 11.3 MPa. The Young's modulus, calculated from the stress–strain curve and averaged over six crystals, is 51.2 ± 24.2 MPa on the (101) face. Although this value may be slightly underestimated due to creep, it provides a realistic approximation of the Young's modulus obtained from a commonly used method for measurement of the macroscopic bulk modulus. It also reflects the pronounced bulk softness of the material. Nanoindentation was also considered to measure

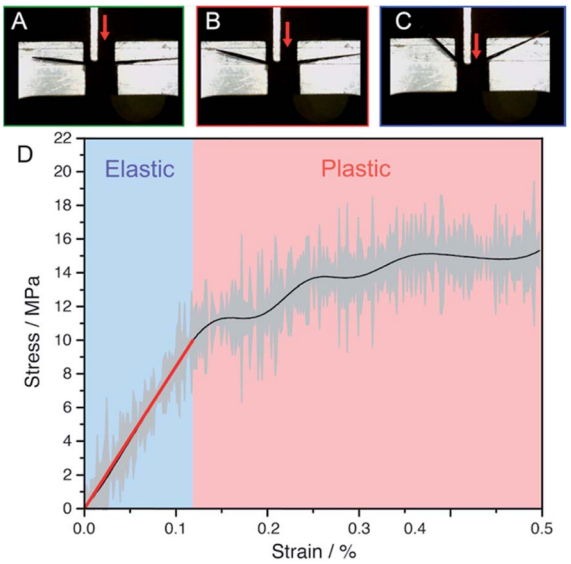

Fig. 3 Mechanical properties of a crystal of **1β**. (A–C) Three optical images of a crystal of **1β** being bent. The red arrows indicate the direction of motion of the jig, which appears as a white/silver line in the upper part of the figure. The crystal appears as black object on the white/silver stage. (D) Stress–strain curve of a single crystal subjected to three-point bending. The equation for the straight red line is $y = 86.3x$ with $R^2 = 0.996$. The red section of the curve indicates the region of the stress–strain curve that was used to calculate the Young's modulus. The error in the measurement is shown as a gray background.

the surface mechanical properties, however, the reactivity of the surface of crystals of **1** to oxygen and water over the long acquisition time required for such measurements resulted in high variance of the measured values. Nevertheless, the approximate value of the modulus above reveals that the crystals of **1β** are very soft, in line with the absence of strong intermolecular interactions in their structure. Such softness is characteristic and common for other plastically bendable crystals.[16,48,49] The variance in the measurement comes from the natural imperfections and defects found in the crystals, as they create points of weakness in the structure and facilitate bending.

The DTDA **1** is one of the few DTDA radicals that exists as a monomer in the solid state and does not dimerize *via* an interaction between singly occupied molecular orbitals to yield a spin-paired diamagnetic material, as is commonly observed for DTDAs.[39] When a crystal of **1β** is bent, its concave (inner) portion is naturally compressed and the convex (outer) area expands. We were curious to see if the rearrangement of radicals occurring during this compression and expansion may result in partial dimerization of the neighboring radicals. To investigate the effect of this mechanical deformation on the number of spins, quantitative EPR and EPR imaging measurements were performed on the crystal before and after bending (Fig. 4). EPR imaging is a technique that detects the number of spins in a three-dimensional volume of space and displays this as a two-dimensional image such that the *z*-dimension of the volume is summed and projected onto the *xy* plane. This results

in a higher relative intensity in thicker portions of the crystal because of the higher amount of material in these regions, leading to a larger sum over z.

A preliminary routine EPR measurement on the pristine single crystal (Fig. 4A; the thickest part of the selected crystal was a nucleation site that appears like a knob located at the top of the shaft of the crystal) showed the expected spectrum with $g = 2.0074$ (ESI Fig. S4†).[36] The crystal was then mechanically bent. EPR images were recorded of the unbent and bent crystal of **1β**, and are shown in Fig. 4B and D, where the bright red color in the image indicates a large number of spins in this region. The shaft of the crystal had a fairly uniform thickness. In line with this, the EPR image has a uniform coloration, although the number of spins is lower towards the periphery of the crystal. After the crystal is bent, areas near the kinks appear to have a decreased spin count, implying that spin-pairing had occurred in these regions due to formation of the diamagnetic dimer. To verify whether there was a decrease in the overall spin count of the sample after bending, quantitative EPR was performed on two separate single crystals. Remarkably, this result showed an increase in spins of 15 and 5% in the two attempts (ESI Fig. S5†). The total spin count of the sample was also measured before and after manual grinding of the crystals, revealing a 5 and 12% increase in the spin count on grinding, respectively. Previous reports[50,51] have described an increase in paramagnetism on grinding for related radicals. In one case,[51] the authors suggested that the increase in paramagnetism was related to a change in associations between radical units on grinding, inducing a second-order phase transition observed by powder X-ray diffraction (PXRD). It was proposed that these changes lead to decreased antiferromagnetic coupling, although a crystal structure that would confirm this hypothesis could not be determined. Using PXRD, which in case of these crystals is known to provide diffraction patterns with pronounced preferred orientation,[31] we have confirmed that no significant structural change occurs on grinding or bending of **1β** (ESI Fig. S6†).

During our work with **1β**, we also noticed that small crystalline impurities of elemental sulfur occasionally appear on the surface of the crystals (ESI Fig. S7†). Sulfur sublimes under the same conditions as **1**[52] and trace amounts of it nucleate on defect sites in crystals of **1β**. Sulfur is known to undergo radical polymerization at elevated temperatures.[52] In order to exclude the possibility that it may also form radicals during application of mechanical pressure, the EPR spectrum of sulfur crystals grown from carbon disulfide was acquired before and after grinding. No change in the signal was detected on grinding, confirming that sulfur impurities are not the source of the increased paramagnetism that was observed on grinding **1β**. An alternative explanation for the increase in paramagnetism on bending or grinding must therefore be sought.

Closer inspection of the EPR imaging results (Fig. 4) reveals that the concave part of the bent section of the crystal shows a decreased EPR signal, while there is remaining signal at the convex region. From the crystal structure of **1β** it is clear that each radical forms four S–N contacts between DTDA rings, which have been shown to be the relevant interactions for magnetic exchange.[36] The strength of the antiferromagnetic exchange interaction is directly related to the geometry of these contacts, as shown by Deumal *et al.*[35] As the crystal is cooled, there is contraction of the unit cell, and the relevant magnetic exchange term J becomes more negative. A study of **1β** at high pressure showed a linear increase in the magnitude of J with increasing pressure.[32] This is related to a decrease in S–N contact distances, and a change in the angle of the aryl ring with respect to the DTDA ring towards 90°. It is clear that a change in the S–N contact distance affects the magnitude of the antiferromagnetic exchange interaction.[53,54]

At ambient temperature and pressure the S–N contact is 3.521(2) Å and the magnetic exchange interaction J is computed to be -26 cm^{-1}. At 5.2 kbar, the S–N contact reduces to 3.344(2) Å, and J is -49.4 cm^{-1}.[33] A more negative J indicates stronger antiferromagnetic interactions and thus an overall decrease in paramagnetism of the sample. We observe an increase in paramagnetism of the sample on bending (and grinding), implying a decrease in the absolute value of J (*i.e.* a less negative J), and an increase in the average S–N contact distance. Defect formation on bending or grinding could also result in reduction in the number of S–N contacts per radical, which would also increase the overall paramagnetism observed in the sample. From the Curie–Weiss law ($\theta = -102$ K), we can estimate the value of χT for **1β** around room temperature at 300 K of approximately 0.280 emu K mol^{-1}. The value of the Weiss

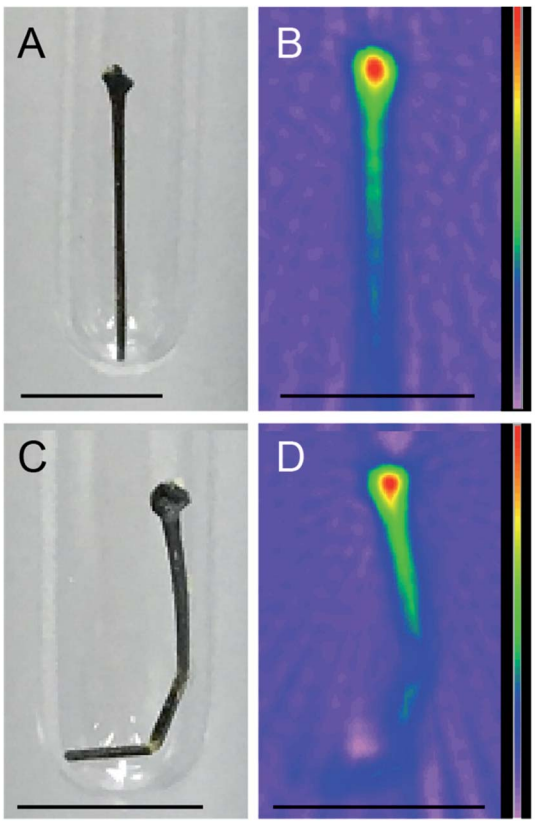

Fig. 4 Effect of bending on the radical count in the crystal of **1**. Optical (A and C) and EPR (B and D) images of a crystal of **1** before (A and B) and after (C and D) bending. The relative intensity in a given area is indicated by color that varies from violet (low) through green to red (high). Scale bar A–D; 5 mm.

constant θ is related to the number of nearest-neighbor interactions, z, by the following relationship:[55]

$$\theta = 2zJS(S + 1)/3k \quad (1)$$

In the case of **1β**, there are four S–N contacts and $z = 4$. If we assume one close contact is broken per radical, *i.e.* each molecule of **1** now only forms three close contacts, the absolute value of θ decreases, and χT increases to 0.299 emu K mol^{-1}. This increase of around 7% is comparable to what we observe experimentally on bending and grinding.

What effect would a small change in S–N contact distances have? According to Thompson *et al.*,[33] the S–N contact distance at room temperature is 3.521(2) Å. Assuming a linear relationship between S–N contact distance and J, the data reported by Thompson *et al.*[33] can be used to show that a 1% increase in this contact distance to 3.556 Å would give $J = -11.5$ cm^{-1}, yielding $\theta = -33$ K. This gives a χT value at room temperature of 0.338, an increase of approximately 20%. Whilst there are several assumptions in this simple model, it is quite clear that very small changes in the S–N contact distance have a significant effect on the paramagnetism of **1β** at room temperature. It is possible that on bending a crystal of **1β**, molecules on the convex side of the kink move further apart, whilst those on the concave side move slightly closer together. This would result in increased spin on the outside of the kink and a decrease in spin on the inside of the kink of the crystal, which is consistent with the EPR imaging (Fig. 4). There will of course be a balance between these two effects, although it is unlikely that they have completely equal contributions. Coupled with an increase in defects (DTDAs forming fewer than four close contacts), this explains the increase in spin observed in samples on bending or grinding. We have also attempted to shed further light on this mechanism by carrying out single-crystal X-ray diffraction experiments on a bent crystal at room temperature, to enable direct comparison to the EPR data, however the experiments did not yield any meaningful results.

Conclusions

We have described the physical and mechanical properties of plastically deformable crystals of a stable radical. The crystals are flexible and bend in two dimensions, achieving plastic flexibility through a common motif of combined strong and weak interactions. This is the first report to show the origin of flexibility using strong S–N interactions and weak F–π interactions along glides planes, and further broadens the scope of intermolecular interactions that can contribute to plasticity in organic crystals. The crystals are exceedingly soft and have a Young's modulus (based on the stress–strain profile) of 51.2 ± 24.2 MPa, similar to other plastic crystals. Remarkably, the crystals were also found to have an increased radical count after bending or grinding, an observation that was rationalized by an increase in S–N interaction distances between adjacent molecules during bending. Moreover, this material adds to the library of plastic crystals and complements other dynamic crystalline materials, such as for example those that can be deformed using light.[56–58] The mechanical compliance of this and other crystals of stable radicals opens prospects for the development of organic magnetoresistance (OMAR) devices based on flexible single crystals.

Author contributions

P. C. carried out the EPR, microscopy and mechanical experiments. P. C. wrote the initial version and edited the manuscript. A. B. D. synthesized the compound, performed initial experiments, and carried out X-ray measurements. L. L. provided additional the X-ray measurements. H. H. performed the EPR measurements. D. A. H. and P. N. inspired the ideas, organized the project, co-wrote and edited the manuscript.

Conflicts of interest

There are no conflicts to declare.

Acknowledgements

We thank New York University Abu Dhabi for financial support for this work. This research was partially carried out using the Core Technology Platform resources at New York University Abu Dhabi. We also acknowledge the National Research Foundation (South Africa) and Stellenbosch University for funding.

Notes and references

1 H. Koshima, *Mechanically responsive materials for soft robotics*, Wiley-VCH, Weinheim, Germany, 2020.
2 I. A. Olson, A. G. Shtukenberg, B. Kahr and M. D. Ward, *Rep. Prog. Phys.*, 2018, **81**, 096501.
3 P. Naumov, D. P. Karothu, A. Ejaz, P. Commins, J. M. Halabi, M. B. Al-Handawi and L. Li, *J. Am. Chem. Soc.*, 2020, **142**, 13256–13272.
4 C. M. Reddy, R. C. Gundakaram, S. Basavoju, M. T. Kirchner, K. A. Padmanabhan and G. R. Desiraju, *Chem. Commun.*, 2005, 3945–3947.
5 C. M. Reddy, M. T. Kirchner, R. C. Gundakaram, K. A. Padmanabhan and G. R. Desiraju, *Chem.–Eur. J.*, 2006, **12**, 2222–2234.
6 C. M. Reddy, K. A. Padmanabhan and G. R. Desiraju, *Cryst. Growth Des.*, 2006, **6**, 2720–2731.
7 P. Commins, D. P. Karothu and P. Naumov, *Angew. Chem., Int. Ed.*, 2019, **58**, 10052–10060.
8 A. Worthy, A. Grosjean, M. C. Pfrunder, Y. Xu, C. Yan, G. Edwards, J. K. Clegg and J. C. McMurtrie, *Nat. Chem.*, 2018, **10**, 65–69.
9 H. Liu, Z. Bian, Q. Cheng, L. Lan, Y. Wang and H. Zhang, *Chem. Sci.*, 2019, **10**, 227–232.
10 A. K. Saini, K. Natarajan and S. M. Mobin, *Chem. Commun.*, 2017, **53**, 9870–9873.
11 S. Hayashi, S.-Y. Yamamoto, D. Takeuchi, Y. Ie and K. Takagi, *Angew. Chem., Int. Ed.*, 2018, **57**, 17002–17008.
12 S. Hayashi and T. Koizumi, *Angew. Chem., Int. Ed.*, 2016, **55**, 2701–2704.

13 S. Hayashi, F. Ishiwari, T. Fukushima, S. Mikage, Y. Imamura, M. Tashiro and M. Katouda, *Angew. Chem., Int. Ed.*, 2020, **59**, 16195–16201.
14 S. R. Anton and H. A. Sodano, *Smart Mater. Struct.*, 2007, **16**, R1–R21.
15 L. Li, P. Commins, M. B. Al-Handawi, D. P. Karothu, J. M. Halabi, S. Schramm, J. Weston, R. Rezgui and P. Naumov, *Chem. Sci.*, 2019, **10**, 7327–7332.
16 P. Commins, M. B. Al-Handawi, D. P. Karothu, G. Raj and P. Naumov, *Chem. Sci.*, 2020, **11**, 2606–2613.
17 E. Ahmed, D. P. Karothu and P. Naumov, *Angew. Chem., Int. Ed.*, 2018, **57**, 8837–8846.
18 Y. Gong, Y. Guo, F. Ge, W. Xiong, J. Su, Y. Sun, C. Zhang, A. M. Cao, Y. Zhang, J. Zhao and Y. Che, *Angew. Chem., Int. Ed.*, 2020, **59**, 10337–10342.
19 E. Ahmed, D. P. Karothu, M. Warren and P. Naumov, *Nat. Commun.*, 2019, **10**, 1–9.
20 D. P. Karothu, J. M. Halabi, L. Li, A. Colin-Molina, B. Rodríguez-Molina and P. Naumov, *Adv. Mater.*, 2020, **32**, e1906216.
21 S. K. Park and Y. Diao, *Chem. Soc. Rev.*, 2020, **49**, 8297–8314.
22 L. Zhu, R. O. Al-Kaysi and C. J. Bardeen, *J. Am. Chem. Soc.*, 2011, **133**, 12569–12575.
23 X. Dong, F. Tong, K. M. Hanson, R. O. Al-Kaysi, D. Kitagawa, S. Kobatake and C. J. Bardeen, *Chem. Mater.*, 2019, **31**, 1016–1022.
24 S. K. Park, H. Sun, H. Chung, B. B. Patel, F. Zhang, D. W. Davies, T. J. Woods, K. Zhao and Y. Diao, *Angew. Chem., Int. Ed.*, 2020, **59**, 13004–13012.
25 L. O. Alimi, P. Lama, V. J. Smith and L. J. Barbour, *Chem. Commun.*, 2018, **54**, 2994–2997.
26 S. Saha and G. R. Desiraju, *Chem. Commun.*, 2017, **53**, 6371–6374.
27 A. Mondal, B. Bhattacharya, S. Das, S. Bhunia, R. Chowdhury, S. Dey and C. M. Reddy, *Angew. Chem., Int. Ed.*, 2020, **59**, 10971–10980.
28 C.-M. Chou, S. Nobusue, S. Saito, D. Inoue, D. Hashizume and S. Yamaguchi, *Chem. Sci.*, 2015, **6**, 2354–2359.
29 H. Liu, Z. Lu, B. Tang, C. Qu, Z. Zhang and H. Zhang, *Angew. Chem., Int. Ed.*, 2020, **59**, 12944–12950.
30 M. K. Panda, S. Ghosh, N. Yasuda, T. Moriwaki, G. D. Mukherjee, C. M. Reddy and P. Naumov, *Nat. Chem.*, 2015, **7**, 65–72.
31 S. P. Thomas, M. W. Shi, G. A. Koutsantonis, D. Jayatilaka, A. J. Edwards and M. A. Spackman, *Angew. Chem., Int. Ed.*, 2017, **56**, 8468–8472.
32 A. J. Banister, N. Bricklebank, W. Clegg, M. R. J. Elsegood, C. I. Gregory, I. Lavendar, J. M. Rawson and B. K. Tanner, *J. Chem. Soc., Chem. Commun.*, 1995, 679–680.
33 R. I. Thompson, C. M. Pask, G. O. Lloyd, M. Mito and J. M. Rawson, *Chem.–Eur. J.*, 2012, **18**, 8629–8633.
34 A. J. Banister, N. Bricklebank, I. Lavender, J. M. Rawson, C. I. Gregory, B. K. Tanner, W. Clegg, M. R. J. Elsegood and F. Palacio, *Angew. Chem., Int. Ed. Engl.*, 1996, **35**, 2533–2535.
35 M. Deumal, J. M. Rawson, A. E. Goeta, J. A. K. Howard, R. C. B. Copley, M. A. Robb and J. J. Novoa, *Chem.–Eur. J.*, 2010, **16**, 2741–2750.
36 A. Alberola, C. M. Pask, J. M. Rawson, E. J. L. McInnes, J. Wolowska, H. El Mkami and G. Smith, *J. Phys. Chem. B*, 2003, **107**, 14158–14160.
37 R. I. Thomson, E. S. L. Wright, J. M. Rawson, C. J. Howard and M. A. Carpenter, *Phys. Rev. B: Condens. Matter Mater. Phys.*, 2011, **84**, 104450.
38 Y. Beldjoudi, A. Arauzo, F. Palacio, M. Pilkington and J. M. Rawson, *J. Am. Chem. Soc.*, 2016, **138**, 16779–16786.
39 D. A. Haynes, *CrystEngComm*, 2011, **13**, 4793–4805.
40 T. Kwon, J. Y. Koo and H. C. Choi, *Angew. Chem., Int. Ed.*, 2020, **59**, 16436–16439.
41 C. G. Pierpont, *Proc.–Indian Acad. Sci., Chem. Sci.*, 2002, **114**, 247–254.
42 G. A. Abakumov and V. I. Nevodchikov, *Dokl. Phys. Chem.*, 1982, **266**, 1407–1410.
43 C. W. Lange, M. Földeàki, V. I. Nevodchikov, V. K. Cherkasov, G. A. Abakumov and C. G. Pierpont, *J. Am. Chem. Soc.*, 1992, **114**, 4220–4421.
44 S. W. Robinson, D. A. Haynes and J. M. Rawson, *CrystEngComm*, 2013, **15**, 10205–10211.
45 P. Li, J. M. Maier, E. C. Vik, C. J. Yehl, D. E. Dial, A. E. Rickher, M. D. Smith, P. J. Pellechia and K. D. Shimizu, *Angew. Chem., Int. Ed.*, 2017, **56**, 7209–7212.
46 S. Bhandary, A. J. Thompson, J. C. McMurtrie, J. K. Clegg, P. Ghosh, S. R. N. K. Mangalampalli, S. Takamizawa and D. Chopra, *Chem. Commun.*, 2020, **56**, 12841–12844.
47 G. R. Krishna, R. Devarapalli, G. Lal and C. M. Reddy, *J. Am. Chem. Soc.*, 2016, **138**, 13561–13567.
48 C. Wang and C. C. Sun, *CrystEngComm*, 2020, **22**, 1149–1153.
49 M. Annadhasan, D. P. Karothu, R. Chinnasamy, L. Catalano, E. Ahmed, S. Ghosh and P. Naumov, *Angew. Chem., Int. Ed.*, 2020, **59**, 13821–13830.
50 G. Antorrena, S. Brownridge, T. S. Cameron, F. Palacio, S. Parsons, J. Passmore, L. K. Thompson and F. Zarlaida, *Can. J. Chem.*, 2002, **80**, 1568–1583.
51 T. S. Cameron, M. T. Lemaire, J. Passmore, J. M. Rawson, K. V. Shuvaev and L. K. Thompson, *Inorg. Chem.*, 2005, **44**, 2576–2578.
52 B. Meyer, *Chem. Rev.*, 1976, **76**, 367–388.
53 C. Rajadurai, V. Enkelmann, G. Zoppellaro and M. Bamugarten, *J. Phys. Chem. B*, 2007, **111**, 4327–4334.
54 C. Rajadurai, O. Fuhr, V. Enkelmann and M. Baumgarten, *J. Phys. Org. Chem.*, 2006, **19**, 257–262.
55 E. L. Gavey and J. M. Rawson, Magnetic measurements, in *Comprehensive Supramolecular Chemistry II*, ed. J. L. Atwood, Elsevier, 2017, pp. 151–180.
56 C. Yang, L. Zhu, R. A. Kudla, J. D. Hartman, R. O. Al-Kaysi, S. Monaco, B. Schatschneider, A. Magalhães, G. J. Beran, C. J. Bardeen and L. J. Mueller, *CrystEngComm*, 2016, **18**, 7319–7329.
57 L. Zhu, F. Tong, N. Zaghloul, O. Baz, C. J. Bardeen and R. O. Al-Kaysi, *J. Mater. Chem. C*, 2016, **4**, 8245–8252.
58 R. O. Al-Kaysi, L. Zhu, M. Al-Haidar, M. K. Al-Muhannah, K. El-Boubbou, T. M. Hamdan and C. J. Bardeen, *CrystEngComm*, 2015, **17**, 8835–8842.